Carbonate record of temporal change in oxygen fugacity and gaseous species in asteroid Ryugu

Wataru Fujiya[1*], Noriyuki Kawasaki[2], Kazuhide Nagashima[3], Naoya Sakamoto[4], Conel M. O'D. Alexander[5], Noriko T. Kita[6], Kouki Kitajima[6], Yoshinari Abe[7], Jérôme Aléon[8], Sachiko Amari[9,10], Yuri Amelin[11], Ken-ichi Bajo[2], Martin Bizzarro[12], Audrey Bouvier[13], Richard W. Carlson[5], Marc Chaussidon[14], Byeon-Gak Choi[15], Nicolas Dauphas[16], Andrew M. Davis[16],Tommaso Di Rocco[17], Ryota Fukai[18], Ikshu Gautam[19], Makiko K. Haba[19], Yuki Hibiya[20], Hiroshi Hidaka[21], Hisashi Homma[22], Peter Hoppe[23], Gary R. Huss[3], Kiyohiro Ichida[24], Tsuyoshi Iizuka[25], Trevor R. Ireland[26], Akira Ishikawa[19], Shoichi Itoh[27], Thorsten Kleine[28], Shintaro Komatani[24], Alexander N. Krot[3], Ming-Chang Liu[29,30], Yuki Masuda[19], Kevin D. McKeegan[29], Mayu Morita[24], Kazuko Motomura[31], Frédéric Moynier[14], Izumi Nakai[32], Ann Nguyen[33], Larry Nittler[5], Morihiko Onose[24], Andreas Pack[17], Changkun Park[34], Laurette Piani[35], Liping Qin[36], Sara S. Russell[37], Maria Schönbächler[38], Lauren Tafla[29], Haolan Tang[29], Kentaro Terada[39], Yasuko Terada[40], Tomohiro Usui[18], Sohei Wada[2], Meenakshi Wadhwa[41], Richard J. Walker[42], Katsuyuki Yamashita[43], Qing-Zhu Yin[44], Tetsuya Yokoyama[19], Shigekazu Yoneda[45], Edward D. Young[29], Hiroharu Yui[46], Ai-Cheng Zhang[47], Tomoki Nakamura[48], Hiroshi Naraoka[49], Takaaki Noguchi[27], Ryuji Okazaki[49], Kanako Sakamoto[18], Hikaru Yabuta[50], Masanao Abe[18], Akiko Miyazaki[18], Aiko Nakato[18], Masahiro Nishimura[18], Tatsuaki Okada[18], Toru Yada[18], Kasumi Yogata[18], Satoru Nakazawa[18], Takanao Saiki[18], Satoshi Tanaka[18], Fuyuto Terui[51], Yuichi Tsuda[18], Sei-ichiro Watanabe[21], Makoto Yoshikawa[18], Shogo Tachibana[52], and Hisayoshi Yurimoto[2]

*Corresponding author (wataru.fujiya.sci@vc.ibaraki.ac.jp)

Affiliations:

[1]Faculty of Science, Ibaraki University; Mito 310-8512, Japan.

[2]Department of Natural History Sciences, Hokkaido University; Sapporo 060-0810, Japan.

[3]Hawai‘i Institute of Geophysics and Planetology, University of Hawai‘i at Mānoa; Honolulu, HI 96822, USA.

[4]Isotope Imaging Laboratory, Creative Research Institution, Hokkaido University; Sapporo 001-0021, Japan.

[5]Earth and Planets Laboratory, Carnegie Institution for Science; Washington, DC, 20015, USA.

[6]Geoscience, University of Wisconsin- Madison; Madison, WI 53706, USA.

[7]Graduate School of Engineering Materials Science and Engineering, Tokyo Denki University; Tokyo 120-8551, Japan.

[8]Institut de Minéralogie, de Physique des Matériaux et de Cosmochimie, Sorbonne Université,

Museum National d'Histoire Naturelle, CNRS UMR 7590, IRD; 75005 Paris, France.
[9]McDonnell Center for the Space Sciences and Physics Department, Washington University; St. Louis, MO 63130, USA.
[10]Geochemical Research Center, The University of Tokyo; Tokyo 113-0033, Japan.
[11]Guangzhou Institute of Geochemistry, Chinese Academy of Sciences; Guangzhou, GD 510640, China.
[12]Centre for Star and Planet Formation, GLOBE Institute, University of Copenhagen; Copenhagen, K 1350, Denmark.
[13]Bayerisches Geoinstitut, Universität Bayreuth; Bayreuth 95447, Germany.
[14]Université Paris Cité, Institut de physique du globe de Paris, CNRS; 75005 Paris, France
[15]Department of Earth Science Education, Seoul National University; Seoul 08826, Republic of Korea.
[16]Department of the Geophysical Sciences and Enrico Fermi Institute, The University of Chicago, 5734 South Ellis Avenue, Chicago 60637, USA.
[17]Faculty of Geosciences and Geography, University of Göttingen; Göttingen, D-37077, Germany.
[18]ISAS/JSEC, JAXA; Sagamihara 252-5210, Japan.
[19]Department of Earth and Planetary Sciences, Tokyo Institute of Technology; Tokyo 152-8551, Japan.
[20]General Systems Studies, The University of Tokyo; Tokyo 153-0041, Japan.
[21]Earth and Planetary Sciences, Nagoya University; Nagoya 464-8601, Japan.
[22]Osaka Application Laboratory, SBUWDX, Rigaku Corporation; Osaka 569-1146, Japan.
[23]Max Planck Institute for Chemistry; Mainz 55128, Germany.
[24]Analytical Technology, Horiba Techno Service Co., Ltd.; Kyoto 601-8125, Japan.
[25]Earth and Planetary Science, The University of Tokyo; Tokyo 113-0033, Japan.
[26]School of Earth and Environmental Sciences, The University of Queensland; St Lucia QLD 4072, Australia.
[27]Earth and Planetary Sciences, Kyoto University; Kyoto 606-8502, Japan.
[28]Max Planck Institute for Solar System Research; 37077 Göttingen, Germany.
[29]Earth, Planetary, and Space Sciences, UCLA; Los Angeles, CA 90095, USA.
[30]Lawrence Livermore National Laboratory; Livermore, CA 94550, USA.
[31]Thermal Analysis, Rigaku Corporation; Tokyo 196-8666, Japan.
[32]Applied Chemistry, Tokyo University of Science; Tokyo 162-8601, Japan.
[33]Astromaterials Research and Exploration Science, NASA Johnson Space Center; Houston, TX 77058, USA.
[34]Earth-System Sciences, Korea Polar Research Institute; Incheon 21990, Korea.
[35]Centre de Recherches Pétrographiques et Géochimiques, CNRS - Université de Lorraine; 54500 Nancy, France.
[36]University of Science and Technology of China, School of Earth and Space Sciences; Anhui 230026,

China.
[37]Department of Earth Sciences, Natural History Museum; London, SW7 5BD, UK.
[38]Institute for Geochemistry and Petrology, Department of Earth Sciences, ETH Zurich; Zurich, Switzerland.
[39]Earth and Space Science, Osaka University; Osaka 560-0043, Japan.
[40]Spectroscopy and Imaging, Japan Synchrotron Radiation Research Institute; Hyogo 679-5198 Japan.
[41]School of Earth and Space Exploration, Arizona State University; Tempe, AZ 85281, USA.
[42]Geology, University of Maryland; College Park, MD 20742, USA.
[43]Graduate School of Natural Science and Technology, Okayama University; Okayama 700-8530, Japan.
[44]Earth and Planetary Sciences, University of California; Davis, CA 95616, USA.
[45]Science and Engineering, National Museum of Nature and Science; Tsukuba 305-0005, Japan.
[46]Chemistry, Tokyo University of Science; Tokyo 162-8601, Japan.
[47]School of Earth Sciences and Engineering, Nanjing University; Nanjing 210023, China.
[48]Department of Earth Science, Tohoku University; Sendai, 980-8578, Japan.
[49]Department of Earth and Planetary Sciences, Kyushu University; Fukuoka 819-0395, Japan.
[50]Earth and Planetary Systems Science Program, Hiroshima University; Higashi-Hiroshima, 739-8526, Japan.
[51]Kanagawa Institute of Technology; Atsugi 243-0292, Japan.
[52]UTokyo Organization for Planetary and Space Science, University of Tokyo; Tokyo 113-0033, Japan.

The Hayabusa2 spacecraft explored asteroid 162173 Ryugu and brought its surface materials to Earth. Ryugu samples resemble Ivuna-type (CI) chondrites – the most chemically primitive meteorites – and contain secondary phyllosilicates and carbonates, which are indicative of aqueous alteration. Understanding the conditions (such as temperature, redox conditions, and fluid composition) during aqueous alteration is crucial to elucidating how Ryugu evolved to its present state, but little is known about the temporal changes in these conditions. Here we show that calcium carbonate (calcite) grains in Ryugu and Ivuna samples have variable $^{18}O/^{16}O$ and $^{13}C/^{12}C$ ratios that are respectively 24–46‰ and 65–108‰ greater than terrestrial standard values, whereas those of calcium-magnesium carbonate (dolomite) grains are much more homogeneous, ranging within 31–36‰ for oxygen and 67–75‰ for carbon. We infer that the calcite precipitated first over a wide range of temperatures and oxygen partial pressures, and that the proportion of gaseous CO_2/CO/CH_4 molecules changed temporally. By contrast, the dolomite formed later in a more oxygen-rich and thus CO_2-dominated environment when the system was approaching equilibrium. The characteristic isotopic compositions of secondary carbonates in Ryugu and Ivuna are not observed for other hydrous meteorites, suggesting a unique evolutionary pathway for these asteroids.

The Japan Aerospace Exploration Agency (JAXA) Hayabusa2 spacecraft explored the near-Earth asteroid 162173 Ryugu and brought samples of its surface materials back to Earth[1,2]. Ryugu has been classified spectroscopically as a member of the C-complex of asteroids[3,4]. It is a rubble pile asteroid consisting of numerous rocky blocks that are the fragments resulting from the disruption of an original, larger parent body[5-7].

Previous work has reported that Ryugu materials underwent extensive aqueous alteration as the result of water activity in the original parent body[8-10] and are mainly composed of secondary minerals that formed during the aqueous alteration: phyllosilicates, carbonates, sulphides, and oxides. On the other hand, primary minerals like anhydrous silicates are rare[9]. These petrological characteristics are comparable to those in the CI (Ivuna-type) chondritic meteorites, pointing to a kinship between Ryugu and CI chondrites. The Ryugu's whole-rock chemical and isotope compositions confirm a close affinity with CI chondrites[8,11,12].

Carbonates, the major Ca budget in Ryugu and CI chondrites[13], are of particular interest because (*i*) their chemical and isotopic compositions reflect the conditions of aqueous alteration, and (*ii*) their grain size is commonly large enough to allow *in-situ* analysis by electron and ion microprobes[14-17]. The C source of carbonates is unclear but was likely ices that included CO, CO_2, and CH_4, and/or organic matter[18,19]. These materials may have formed in the solar nebula or even the parental molecular

cloud of the solar system. Therefore, the C isotope compositions recorded by carbonates can help us shed light on the physicochemical processes that operated in these environments.

In this study, we investigate the conditions of aqueous alteration and the origin of the materials accreted by the Ryugu/CI parent bodies. To this end, we performed *in-situ* O and C isotope measurements of calcite ($CaCO_3$) and dolomite ($CaMg(CO_3)_2$) in Ryugu samples A0058, collected at the first touchdown site, and C0002, from the second touchdown site, as well as the Ivuna meteorite. The O isotope data of the A0058 and Ivuna dolomite are taken from a previous study[8].

Occurrences and isotope compositions of carbonate minerals

Dolomite is the most abundant carbonate mineral in the analysed samples, and we found numerous dolomite grains throughout the Ryugu and Ivuna matrices, whereas calcite is rare. No calcite grains were observed in the Ryugu A0058 sample studied. Calcite was found only in limited areas (clasts) of the Ryugu C0002 and Ivuna samples, occurring with primary anhydrous silicate minerals like Mg-rich olivine and pyroxene (Fig. 1a). The calcite grains (<10 μm in size) are usually smaller than the dolomite grains (several tens of μm) (Fig. 1b). The dolomite has compositional variation and complex zoning within grains (Extended Data Fig. 1). We also found breunnerite ($Mg(Fe,Mn)(CO_3)_2$) grains, for which we did not measure isotope compositions because of the lack of a suitable standard material for isotope analysis.

The O and C isotope compositions of the Ryugu and Ivuna carbonates are similar (Table 1). The $\delta^{18}O$ values of the calcite in C0002 and Ivuna (+24 to +46‰) show a grain-to-grain variation larger than those of the dolomite in C0002, A0058, and Ivuna (+26 to +31‰) ($\delta^{i}O$ in ‰ = $[(^{i}O/^{16}O)_{sample}/(^{i}O/^{16}O)_{VSMOW} - 1] \times 1000$; i = 17 or 18 and VSMOW is the terrestrial standard material, Vienna standard mean ocean water) (Fig. 2a). The simple average of the $\Delta^{17}O$ values, the deviation from the terrestrial fractionation line defined as $\Delta^{17}O = \delta^{17}O - 0.52 \times \delta^{18}O$, of the C0002 and Ivuna calcite is +1.37 ± 0.40‰ (2SE, N = 17). The $\Delta^{17}O$ values of the C0002, A0058, and Ivuna dolomite are systematically lower than those of the calcite, and the average $\Delta^{17}O$ value of the dolomite (+0.26 ± 0.23‰, 2SE, N = 16) is closer to the whole-rock values of three Ryugu samples[8] (+0.61 ± 0.28‰, 2SD; Fig. 2b). The previously measured O isotope compositions of the A0058 and Ivuna dolomite are in good agreement with those of the C0002 dolomite measured in this study[8].

Like the $\delta^{18}O$ values, the dolomite in A0058, C0002, and Ivuna has a relatively narrow range of $\delta^{13}C$ values from +67 to +75‰ ($\delta^{13}C$ in ‰ = $[(^{13}C/^{12}C)_{sample}/(^{13}C/^{12}C)_{VPDB} - 1] \times 1000$; VPDB is the terrestrial standard material, Vienna Pee Dee belemnite) (Fig. 3). The $\delta^{13}C$ and $\delta^{18}O$ values of the dolomite are broadly consistent with the bulk $\delta^{13}C$ and $\delta^{18}O$ values of carbonates, including calcite,

dolomite, and breunnerite, in CI chondrites (Ivuna and Orgueil) determined on whole-rock samples[18], corroborating the observation that dolomite is the major carbonate mineral. On the other hand, the $\delta^{13}C$ values of the calcite in C0002 and Ivuna are highly heterogeneous from grain to grain, ranging from +65 to +108‰, and they are commonly higher than those of the Ryugu and Ivuna dolomite (Fig. 3). These variations have also been reported for other Ryugu samples[20], confirming that our results represent the isotopic characteristics of Ryugu carbonates. For calcite grains on which we conducted multiple measurements, the $\delta^{13}C$ values in each grain are identical within uncertainties of ~5.1‰. Thus, the heterogeneity of $\delta^{13}C$ values within individual calcite grains is likely no larger than 10‰, which is much smaller than the heterogeneity of >40‰ between grains.

Isotope signatures of the Ryugu and CI carbonates

If the carbonates were in O and C isotopic equilibrium with the aqueous fluid when they precipitated, their O and C isotope compositions would have been determined by the mass dependent equilibrium isotopic fractionation between carbonates and water for O, and that between carbonates and dissolved CO_3^{2-} (and other dissolved C-bearing chemical species) for C. The magnitude of this equilibrium isotopic fractionation depends on temperature[21]. Thus, the O and C isotope compositions of the carbonates would reflect those of water and CO_3^{2-} as well as their formation temperatures. Assuming equilibrium, the temperature of dolomite-magnetite precipitation in the Ryugu A0058 sample analysed previously is estimated to be 37 ± 10 °C (ref.[8]), while the inferred alteration temperatures of CI chondrites range up to 150 °C (ref.[22]). The equilibrium O isotopic fractionation between water and calcite leads to the enhancement of $\delta^{18}O$ values in calcite relative to water by approximately +38, +28 and +13‰ at 0, 40, and 150 °C, respectively[23]. Thus, the $\delta^{18}O$ variation of ~22‰ observed in the Ryugu calcite (Fig. 2) is potentially explained by formation temperatures that varied from 0 to 150 °C assuming a fixed $\delta^{18}O$ value of water.

However, this argument does not necessarily mean that variable formation temperature is the sole explanation for the observed $\delta^{18}O$ variation of the calcite. Indeed, the lack of a simple correlation between $\delta^{18}O$ and $\delta^{13}C$ values (Fig. 3) implies that variable formation temperatures alone cannot explain the observed $\delta^{18}O$ and $\delta^{13}C$ variations because the $\delta^{18}O$ and $\delta^{13}C$ values of carbonates should co-vary with their formation temperatures[18]. Rather it seems likely that the $\delta^{18}O$ value of water and/or the $\delta^{13}C$ value of CO_3^{2-} varied spatially and/or temporally. A previous study used clumped isotope thermometry for carbonates in Mighei-type (CM) chondrites and demonstrated that the $\delta^{18}O$ values of water are variable between samples[16].

Mass balance calculations[24,25] and the O isotope composition of the putative, early solar system water[26,27] suggest that prior to the onset of alteration, water in the CI and other carbonaceous chondrites

had a significantly higher $\Delta^{17}O$ value, and possibly $\delta^{18}O$ value, than the anhydrous silicates[28]. Thus, as alteration progressed, the $\Delta^{17}O$ value, and possibly the $\delta^{18}O$ value, of the altering fluid would have decreased[24,25]. The $\Delta^{17}O$ values of the carbonates and fluid will be identical at equilibrium, and thus, the $\Delta^{17}O$ values of the carbonates are a measure of the degree of progress of water-rock interactions. The $\Delta^{17}O$ values of the dolomite in the Ryugu and Ivuna samples are systematically lower than those of the calcite, and the Ryugu and Ivuna carbonates show resolvable $\Delta^{17}O$ variations beyond uncertainties (Fig. 2b). Therefore, the calcite with systematically higher $\Delta^{17}O$ values formed from less "evolved" fluids, and crystallized earlier than the dolomite. The fact that calcite is more prevalent in less-altered areas, as shown by primary anhydrous silicates, suggests that Ca was more easily leached during incipient aqueous alteration than Mg, allowing the formation of calcite before dolomite.

Like O isotopes, the C isotope compositions of carbonates are determined not only by their formation temperatures but also by the $\delta^{13}C$ values of dissolved CO_3^{2-}. The C isotope composition of CO_3^{2-} could have varied due to (*i*) Rayleigh-type isotopic fractionation as a result of the preferential escape of ^{12}C-rich gaseous species like CH_4 (ref.[16]), (*ii*) the progressive formation of carbonates, i.e., fractional crystallization, (*iii*) the mixing of two or more C reservoirs with distinct $\delta^{13}C$ values that supplied CO_3^{2-} (ref.[19]), and (*iv*) the change in the chemical speciation of the C-bearing gaseous species, such as CO_2, CO, and CH_4, due to varying O and H partial pressures. Rayleigh-type isotopic fractionation was not the primary mechanism for producing the observed $\delta^{13}C$ variation because it would have resulted in higher $\delta^{13}C$ values in the dolomite, which formed from the more evolved fluids than the calcite, whereas the opposite is observed. The influence of fractional crystallization during carbonate formation was also minimal because the rare calcite that formed early presumably when a larger CO_3^{2-} pool was available displays a larger $\delta^{13}C$ variation than the more common dolomite, which is opposite to what one would expect in this scenario.

A previous study advocated that the observed $\delta^{13}C$ variation resulted from the mixing of C reservoirs with distinct $\delta^{13}C$ values reflecting the spatially heterogenous distribution of different C reservoirs[19]. Possible C reservoirs include C-bearing gaseous species such as CO_2, CO, and CH_4, originally accreted in ices, and organic matter, and the previous study invoked CO_2-bearing ices as a ^{13}C-rich reservoir[19]. However, the mixing timescales of gaseous species in the Ryugu/CI parent asteroids would have been short unless the permeability was extremely low. Therefore, the spatially heterogeneous distribution of C reservoirs would have not persisted for long. Furthermore, it is unclear why the calcite has commonly higher $\delta^{13}C$ values than the dolomite, and calcite with lower $\delta^{13}C$ values is generally absent.

Temporal change in oxygen fugacity and gaseous species

Instead of spatial heterogeneity, the temporal variation in the $\delta^{13}C$ values of the C reservoirs and their

chemical speciation likely occurred due to a change in O partial pressure, or more precisely, O fugacity (fO_2), which is O partial pressure corrected for nonideal gas behaviour. Oxygen fugacity varied along with the production of H_2 via the oxidation of Fe in metal and silicates by H_2O and the subsequent escape of H_2 from the system, perhaps by diffusion or by making fractures in the parent body[29]. Thus, fO_2 was determined by the relative rates of the production and escape of H_2; in this scenario, fO_2 would have at first decreased and then increased. In the case of CM chondrites, the amount of Fe^{3+} in their matrices increases with increasing alteration[30], which is in line with this scenario.

The Fe and Mn abundances of terrestrial carbonates that reflect the Fe^{2+} and Mn^{2+} activities in fluids have been used to infer the redox conditions under which they precipitated[31]. However, the Fe and Mn abundances of Ryugu and Ivuna carbonates were likely controlled not only by redox conditions but also by the amounts of these cations leached from primary minerals during the progressive aqueous alteration[32]. Therefore, the zoning of Fe and Mn observed in the dolomite grains may not be a direct proxy for the temporal change in fO_2. Instead, here we propose that the $\delta^{13}C$ values of Ryugu and Ivuna carbonates represent a record of such temporal fO_2 variation.

To see how the $\delta^{13}C$ values of carbonates will change with varying fO_2, we consider a rather simple model, where gaseous CO_2 and CO and carbonates (and dissolved CO_2, HCO_3^-, and CO_3^{2-}) are in C isotopic equilibrium, and the CO_2/CO ratio increases, corresponding to an increase in fO_2. In cometary ices, CO_2 and CO are the most abundant C-bearing chemical species[33], and the Ryugu/CI parent bodies would have accreted significant amounts of CO_2- and CO-bearing ices if they formed in the distal solar system[11,28]. At the earliest stage of aqueous alteration, the CO_2/CO ratio may have been characterized by that of the accreted ices, which may be around unity or higher as observed for cometary ices[33,34]. We assume that the $\delta^{13}C$ value of the bulk gas (CO_2 + CO), $\delta^{13}C_{bulk}$, is constant regardless of the CO_2/CO ratio. Then, the $\delta^{13}C_{bulk}$ is given by mass balance as $\delta^{13}C_{bulk} = x\,\delta^{13}C_{CO2} + (1 - x)\,\delta^{13}C_{CO}$, where x is the mole fraction of CO_2 defined by $x = CO_2/(CO_2 + CO)$, $\delta^{13}C_{CO2}$ and $\delta^{13}C_{CO}$ are the $\delta^{13}C$ values of CO_2 and CO, respectively. Thus, using Δ defined by $\delta^{13}C_{CO2} - \delta^{13}C_{CO}$, $\delta^{13}C_{CO2}$ and $\delta^{13}C_{CO}$ are given by $\delta^{13}C_{CO2} = \delta^{13}C_{bulk} + (1 - x)\,\Delta$ and $\delta^{13}C_{CO} = \delta^{13}C_{bulk} - x\,\Delta$, respectively. The Δ value is approximated by 1000 lnα, where α is the C isotopic fractionation factor between CO_2 and CO defined by $(^{13}C/^{12}C)_{CO2}/(^{13}C/^{12}C)_{CO}$ and is positive at all temperatures (+93, +76, and +48‰ at 0, 40, and 150 °C, respectively[21,35]). Therefore, with increasing x (and fO_2), both the $\delta^{13}C$ values of CO_2 and CO will decrease monotonically, and the $\delta^{13}C$ values of carbonates will also decrease. Thus, in this simple model, a $\delta^{13}C$ variation of carbonates comparable to the observation (~40‰) is expected if the x value varies from 0.5 to 1 (Fig. 3). The redox states evolved within a few million years after the birth of the solar system as inferred from the ^{53}Mn-^{53}Cr chronometry of Ryugu/CI dolomite[8,10,20,36]. The presence of CH_4, another possible reducing gas, does not change this conclusion because the

behaviour of CH_4 in terms of C isotopic fractionation against CO_2 is quite similar to that of CO (ref.[21]). Our model where CO_2 and CO are in C isotopic equilibrium at low temperatures requires the presence of as yet unidentified processes/catalysts. The isotopic equilibrium in thermally matured natural gases has been recently discussed[37].

The characteristic $\delta^{13}C$ values of Ryugu and Ivuna carbonates are not observed for other aqueously altered meteorites such as CM chondrites and the ungrouped carbonaceous chondrite Tagish Lake[19,38,39], suggesting that the redox conditions as well as the thermal history and accreted materials are unique to their parent bodies. For instance, the $\delta^{13}C$ values of CM calcite are variable like Ryugu/CI calcite, but the highest reported value (~+80‰) in CM calcite is lower than that of Ryugu/CI calcite (+108‰) (Extended Data Fig. 2). Furthermore, the $\delta^{13}C$ values of CM dolomite are also variable from ~+40 to ~+60‰, which is in contrast to the homogeneous $\delta^{13}C$ values observed for Ryugu/CI dolomite. Iron in CI chondrites is dominated by octahedral Fe^{3+} and indicates more oxidized conditions than CM chondrites[30], which is consistent with the homogeneous $\delta^{13}C$ values of Ryugu/CI dolomite.

Because the $\delta^{13}C$ values of the Ryugu/CI dolomite are commonly lower and more homogeneous than those of the calcite, the dolomite likely formed at higher fO_2 and/or temperature than the calcite. This, combined with the O isotope signatures of the carbonates, implies that the calcite formed during prograde alteration over wide ranges of fO_2 and temperature, whereas the dolomite formed later during retrograde cooling when the aqueous fluids and silicates approached O isotopic equilibrium. Therefore, when the dolomite formed, the fO_2 was likely high enough that the major gaseous C reservoir was CO_2 (i.e., $x \sim 1$). If correct, the $\delta^{13}C$ value of CO_2 in C isotopic equilibrium with the dolomite, which has the average $\delta^{13}C$ value of ~+70‰, would equal the $\delta^{13}C$ value of the bulk gas. Using the C isotopic fractionation factor between dolomite and CO_2, $(^{13}C/^{12}C)_{dolomite}/(^{13}C/^{12}C)_{CO2}$, of ~1.0092 at 40 °C or ~0.9951 at 150 °C (refs.[40,41]), the $\delta^{13}C_{bulk}$ (= $\delta^{13}C_{CO2}$) value is estimated to be between +61‰ and +75‰.

The above simple model implies a $\delta^{13}C$ value higher than +60‰ for C-bearing molecules originally accreted in ices. Such ^{13}C-rich compositions are not common among solar system materials other than meteoritic carbonates and water-soluble organic compounds[42]. A similar level of ^{13}C-enrichment ($\delta^{13}C$ = +65 ± 51‰), albeit with large uncertainty, has been reported for CO_2 in the coma of 67P/Churyumov-Gerasimenko[43]. The mechanism to produce ^{13}C-rich compositions is not well understood, but self-shielding during CO photodissociation in the solar nebula or the parent molecular cloud of the solar system is a possible mechanism[44-46]. Thus, the inferred ^{13}C-rich composition of C-bearing molecular ices would have resulted from such physicochemical reactions[47,48], and we concluded that the Ryugu/CI parent bodies accreted materials that originated from these cold environments.

Acknowledgements

We thank Drae Rogers, Michael Spicuzza, and John Valley for the preparation of carbonate standard materials for SIMS measurements, and Akira Tsuchiyama for discussion. Hayabusa2 was developed and built under the leadership of Japan Aerospace Exploration Agency (JAXA), with contributions from the German Aerospace Center (DLR) and the Centre National d'Études Spatiales (CNES), and in collaboration with NASA, and other universities, institutes, and companies in Japan. The curation system was developed by JAXA in collaboration with companies in Japan. This research was supported in part by the JSPS KAKENHI grant numbers 19H00725 and 20K20934 to W.F. and T.N.

Author contributions

W.F., N.K., K.N., N.S, and H.Y. designed this study and analysed the samples. W.F., N.K., K.N., C.A., and H.Y. were involved in data reduction and data interpretation. W.F. wrote the paper with support and approval of all co-authors.

Competing interests

The authors declare no competing interests.

Table 1. $\delta^{18}O$, $\delta^{17}O$, $\Delta^{17}O$, and $\delta^{13}C$ values of carbonates in Ryugu and Ivuna samples.

Samples	$\delta^{18}O$ (‰)	2σ	$\delta^{17}O$ (‰)	2σ	$\Delta^{17}O$ (‰)	2σ	$\delta^{13}C$ (‰)	2σ
			Ryugu C0002, calcite					
Calcite#1a	*23.5*	*0.8*	*12.5*	*1.6*	*0.2*	*1.5*	*98.1*	*4.9*
Calcite#1b	*23.5*	*0.8*	*12.5*	*1.6*	*0.2*	*1.5*	*92.7*	*4.8*
Calcite#1ave.	23.5	0.8	12.5	1.6	0.2	1.5	95.4	3.4
Calcite#2	38.4	0.6	22.2	1.1	2.2	1.1	101.7	4.8
Calcite#3-1	44.3	0.8	24.6	1.4	1.6	1.5	89.9	5.2
Calcite#3-2a	*46.3*	*0.8*	*25.9*	*1.6*	*1.9*	*1.7*	*76.2*	*5.7*
Calcite#3-2b	*46.3*	*0.8*	*25.9*	*1.6*	*1.9*	*1.7*	*84.5*	*6.5*
Calcite#3-2c	*46.3*	*0.8*	*25.9*	*1.6*	*1.9*	*1.7*	*81.0*	*5.9*
Calcite#3-2ave.	46.3	0.8	25.9	1.6	1.9	1.7	80.6	3.5
Calcite#3-3	44.5	1.2	24.9	1.5	1.8	1.4	84.1	6.2
Calcite#3-4	42.9	1.2	23.3	1.3	1.0	1.4	87.0	5.6
Calcite#4-1	n.d.		n.d.		n.d.		88.2	5.2
Calcite#4-2	n.d.		n.d.		n.d.		86.1	4.8
Calcite#5a	*41.1*	*1.2*	*24.2*	*1.4*	*2.9*	*1.4*	*93.9*	*4.8*
Calcite#5b	*40.9*	*1.2*	*23.2*	*1.3*	*1.9*	*1.4*	*93.9*	*4.8*
Calcite#5ave.	41.0	0.8	23.7	1.0	2.4	1.0	93.9	4.8
			Ivuna, calcite					
Calcite#1	41.6	1.0	22.5	1.3	0.9	1.4	101.5	4.1
Calcite#2	41.5	1.0	23.4	1.3	1.8	1.4	104.8	4.8
Calcite#3	40.7	1.1	21.9	1.6	0.8	1.4	107.1	4.7
Calcite#5	33.9	1.0	20.0	1.3	2.4	1.4	81.4	3.8
Calcite#6	41.1	1.0	24.0	1.4	2.6	1.4	103.9	6.0
Calcite#7	38.0	1.0	20.2	1.4	0.4	1.4	98.0	5.1
Calcite#8-1	37.6	1.0	20.6	1.3	1.1	1.4	79.5	4.4
Calcite#8-2	37.0	1.0	20.0	1.3	0.8	1.4	89.0	5.2
Calcite#9a	*36.0*	*1.0*	*20.2*	*1.3*	*1.5*	*1.4*	*106.6*	*5.8*
Calcite#9b	*36.0*	*1.0*	*20.2*	*1.3*	*1.5*	*1.4*	*109.9*	*5.1*
Calcite#9c	*36.0*	*1.0*	*20.2*	*1.3*	*1.5*	*1.4*	*106.7*	*4.8*
Calcite#9ave.	36.0	1.0	20.2	1.3	1.5	1.4	107.8	3.0
Calcite#10a	*43.6*	*0.6*	*22.3*	*1.5*	*−0.4*	*1.4*	*65.4*	*4.7*
Calcite#10b	*40.9*	*0.7*	*21.2*	*1.2*	*−0.1*	*1.2*	*65.4*	*4.7*
Calcite#10ave.	42.2	0.5	21.7	1.0	−0.3	0.9	65.4	4.7

Ryugu A0058, dolomite								
Dolomite#5	*(27.0)*	*(0.9)*	*(14.2)*	*(1.0)*	*(0.2)*	*(0.9)*	*67.7*	*1.5*
Dolomite#5	*(27.0)*	*(0.9)*	*(14.2)*	*(1.0)*	*(0.2)*	*(0.9)*	*67.2*	*1.2*
Dolomite#5ave.	(27.0)	(0.9)	(14.2)	(1.0)	(0.2)	(0.9)	67.5	1.0
Dolomite#2	(29.0)	(1.0)	(15.0)	(1.0)	(0.0)	(0.9)	74.8	1.5
Dolomite#4	(30.0)	(0.9)	(15.8)	(1.0)	(0.2)	(0.9)	72.1	1.3
Dolomite#1	(29.9)	(0.9)	(14.8)	(1.0)	(−0.7)	(0.9)	71.3	1.2
Dolomite#3	(29.5)	(0.8)	(15.7)	(1.0)	(0.4)	(0.9)	74.5	1.5
Ryugu C0002, dolomite								
Dolomite#3a	*27.3*	*1.0*	*15.2*	*1.3*	*1.0*	*0.9*	*72.1*	*1.3*
Dolomite#3b	*28.1*	*1.0*	*14.7*	*1.3*	*0.1*	*0.9*	*72.1*	*1.3*
Dolomite#3ave.	27.7	0.7	14.9	0.9	0.6	0.6	72.1	1.3
Dolomite#4	28.3	1.0	15.3	1.3	0.6	0.9	70.1	1.3
Dolomite#1a	*28.6*	*1.0*	*15.6*	*1.3*	*0.7*	*0.9*	*68.1*	*1.3*
Dolomite#1b	*28.7*	*1.0*	*15.1*	*1.3*	*0.2*	*0.9*	*68.1*	*1.3*
Dolomite#1ave.	28.7	0.7	15.4	0.9	0.5	0.6	68.1	1.3
Dolomite#2a	*26.7*	*1.0*	*14.1*	*1.3*	*0.2*	*0.9*	*69.4*	*1.3*
Dolomite#2b	*27.7*	*1.0*	*14.1*	*1.3*	*−0.3*	*0.9*	*69.5*	*1.3*
Dolomite#2ave.	27.2	0.7	14.1	0.9	0.0	0.6	69.4	0.9
Ivuna, dolomite								
Dolomite#1	(29.0)	(0.7)	(15.6)	(0.8)	(0.5)	(0.9)	68.1	1.3
Dolomite#7	(30.8)	(0.7)	(16.0)	(0.8)	(0.0)	(0.7)	68.6	1.1
Dolomite#6	(29.1)	(0.8)	(15.3)	(0.8)	(0.2)	(0.9)	72.3	1.2
Dolomite#5	(28.8)	(0.8)	(16.3)	(0.8)	(1.3)	(0.9)	67.2	1.2
Dolomite#4	(26.5)	(0.9)	(14.4)	(0.9)	(0.7)	(1.0)	68.3	1.3
Dolomite#2a	*(29.6)*	*(0.9)*	*(15.1)*	*(0.9)*	*(−0.3)*	*(0.8)*	*67.4*	*1.3*
Dolomite#2b	*(29.6)*	*(0.9)*	*(15.1)*	*(0.9)*	*(−0.3)*	*(0.8)*	*65.6*	*1.3*
Dolomite#2c	*(29.6)*	*(0.9)*	*(15.1)*	*(0.9)*	*(−0.3)*	*(0.8)*	*67.4*	*1.3*
Dolomite#2ave.	(29.6)	(0.9)	(15.1)	(0.9)	(−0.3)	(0.8)	66.8	0.7
Dolomite#3	(29.2)	(1.0)	(15.4)	(1.0(	(0.2)	(1.1)	68.8	1.2

n.d.: Not determined.

The O isotope compositions of the Ryugu A0058 and Ivuna dolomite, shown in parentheses, are taken from Yokoyama et al. (2022) (ref.[8])

2σ errors are either external reproducibility (2SD) of standard measurements or internal precision (2SE) of the data within single measurements, whichever is the largest.

In case that we analysed single grains multiple times, as shown in Italic, we averaged the data and calculated the corresponding uncertainties by propagating individual errors.

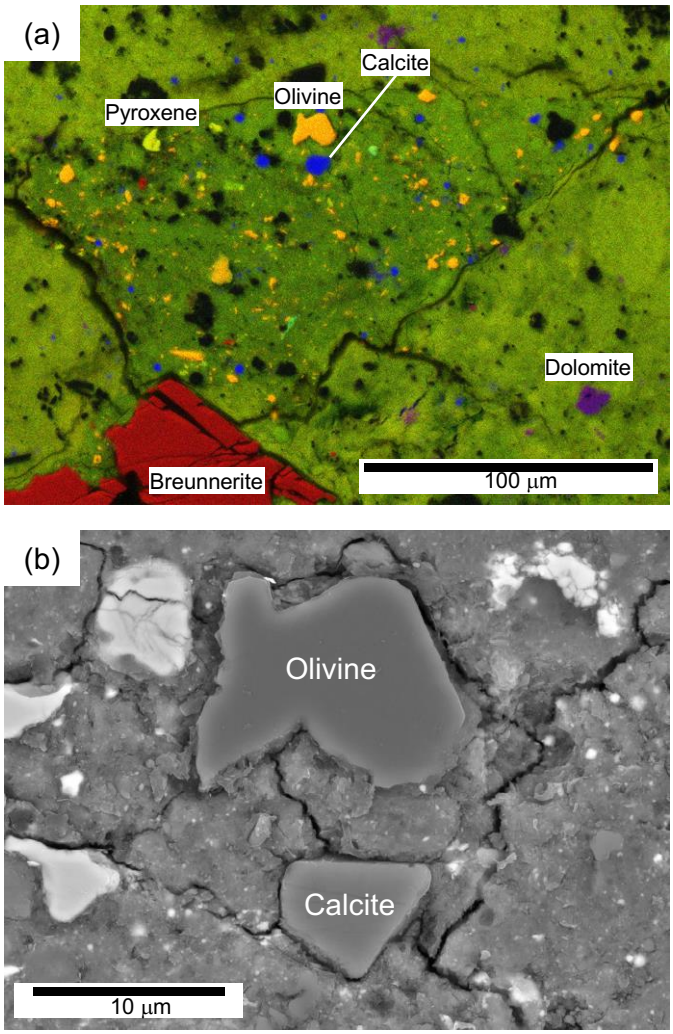

Fig. 1. Calcite grains in the Ryugu C0002 sample. (a) Mg (red), Si (green), and Ca (blue) elemental maps showing the distribution of calcite grains. Calcite grains (blue) in the Ryugu and Ivuna samples can be found in limited areas with Mg-rich olivine (yellow) and pyroxene (light green). Purple grains are dolomite. The large red grain is breunnerite. (b) Backscattered electron image (BEI) of a calcite grain.

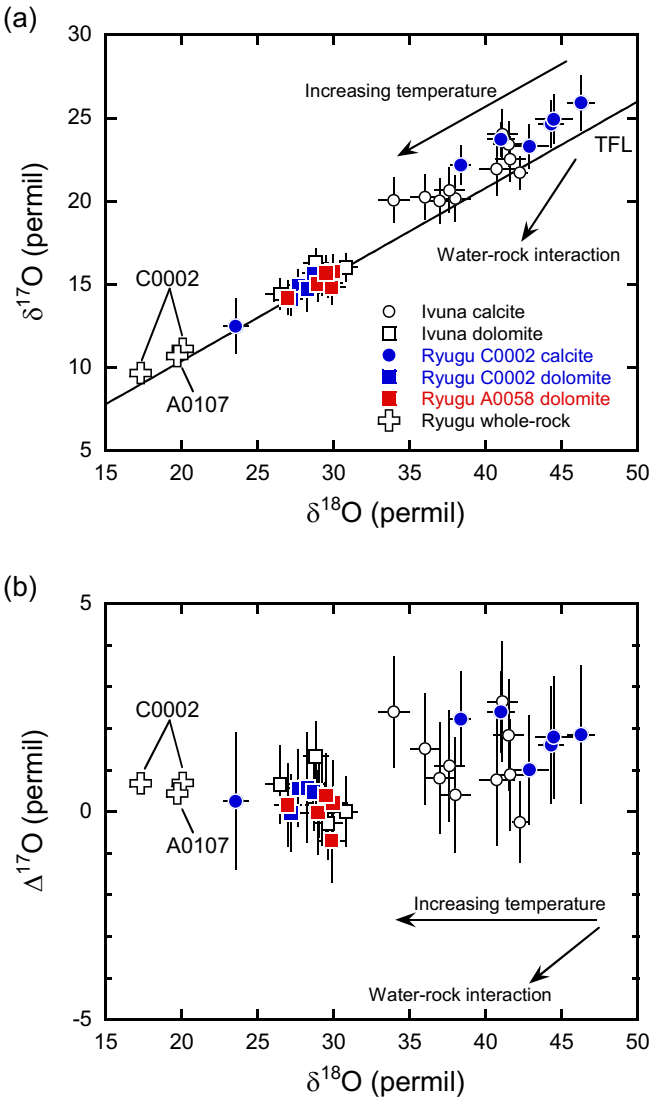

Fig. 2. Oxygen isotope compositions of the calcite and dolomite in Ryugu and Ivuna samples. The whole-rock O isotope compositions of the Ryugu A0107 and C0002 samples are also shown for reference[8]. The changes in O isotope compositions due to variable formation temperatures and water-rock interaction are illustrated by arrows. (a) Oxygen three-isotope plot showing $\delta^{18}O$ vs. $\delta^{17}O$ values. TFL: Terrestrial fractionation line defined as $\delta^{17}O = 0.52 \times \delta^{18}O$. (b) $\delta^{18}O$ vs. $\Delta^{17}O$ values. Data are presented as mean values ± 2σ errors which are either external reproducibility (2SD, N = 6–20 depending on the measurement sessions) of standard measurements or internal precision (2SE) of the data within single measurements, whichever is the largest.

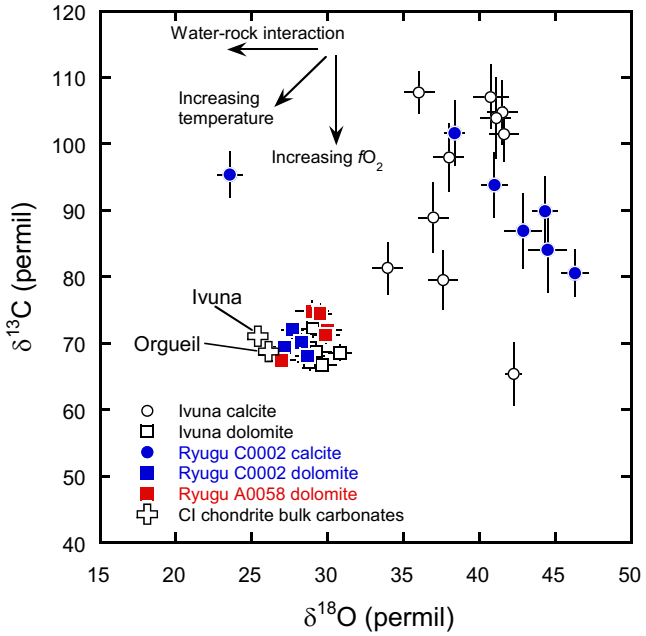

Fig. 3. Comparison between C and O isotope compositions of the calcite and dolomite in Ryugu and Ivuna samples. Errors are 2σ (see also Table 1). The values of carbonates measured for whole-rock CI chondrites (Ivuna and Orgueil) are also shown for reference[18]. The changes in C and O isotope compositions due to variable formation temperatures and O fugacity, and water-rock interaction are illustrated by arrows. The calcite shows much larger variations in both C and O isotope compositions than the dolomite. Note that no simple correlation between $\delta^{13}C$ and $\delta^{18}O$ values can be seen. Data are presented as mean values ± 2σ errors which are either external reproducibility (2SD, N = 6–20 depending on the measurement sessions) of standard measurements or internal precision (2SE) of the data within single measurements, whichever is the largest.

References:

1. Tachibana, S. et al. Hayabusa2: Scientific importance of samples returned from C-type near-Earth asteroid (162173) 1999 JU_3. *Geochem. J.* **48**, 571-587 (2014).
2. Tachibana, S. et al. Pebbles and sand on asteroid (162173) Ryugu: In situ observation and particles returned to Earth. *Science* **375**, 1011-1016 (2022).
3. Binzel, R. P., Harris, A. W., Bus, S. J. & Burbine, T. H. Spectral properties of near-Earth objects: Palomar and IRTF results for 48 objects including spacecraft targets (9969) Braille and (10302) 1989 ML. *Icarus* **151**, 139-149 (2001).
4. Campins, H. et al. Spitzer observations of spacecraft target 162173 (1999 JU3). *Astron. Astrophys.* **503**, L17–L20 (2009).
5. Watanabe, S. et al. Hayabusa2 arrives at the carbonaceous asteroid 162173 Ryugu—A spinning top-shaped rubble pile. *Science* **364**, 268-272 (2019).
6. Sugita, S. et al. The geomorphology, color, and thermal properties of Ryugu: Implications for parent-body processes. *Science* **364**, eaaw0422 (2019).
7. Kitazato K. et al. The surface composition of asteroid 162173 Ryugu from Hayabusa2 near-infrared spectroscopy. *Science* **364**, 272-275 (2019).
8. Yokoyama, T. et al. The first returned samples from a C-type asteroid show kinship to the chemically most primitive meteorites. *Science* **379**, eabn7850 (2022).
9. Nakamura, T. et al. Formation and evolution of carbonaceous asteroid Ryugu: Direct evidence from returned samples. *Science*, 10.1126/science.abn8671 (2022).
10. Nakamura, E. et al. On the origin and evolution of the asteroid Ryugu: A comprehensive geochemical perspective. *Proc. Jpn. Acad., Ser. B* **98**, 227-282 (2022).
11. Hopp, T. et al. Ryugu's nucleosynthetic heritage from the outskirts of the Solar System. *Sci. Adv.* **8**, eadd8141 (2022).
12. Paquet, M. et al. Contribution of Ryugu-like material to Earth's volatile inventory by Cu and Zn isotopic analysis. *Nat. Astron.* **7**, 182-189 (2023).
13. Moynier, F. et al. The Solar System calcium isotopic composition inferred from Ryugu samples. *Geochem. Persp. Let.* **24**, 1-6 (2022).
14. Johnson, C. A. & Prinz, M. Carbonate compositions in CM and CI chondrites, and implications for aqueous alteration. *Geochim. Cosmochim. Acta* **57**, 2843-2852 (1993).
15. Riciputi, L. R., McSween, H. Y. Jr., Johnson, C. A. & Prinz, M. Minor and trace element concentrations in carbonates of carbonaceous chondrites, and implications for the compositions of coexisting fluids. *Geochim. Cosmochim. Acta* **58**, 1343-1351 (1994).
16. Guo, W. & Eiler, J. M. Temperatures of aqueous alteration and evidence for methane generation on the parent bodies of the CM chondrites. *Geochim. Cosmochim. Acta* **71**, 5565-5575 (2007).
17. Verdier-Paoletti, M. J. et al. Oxygen isotope constraints on the alteration temperatures of CM

chondrites. *Earth Planet. Sci. Lett.* 458, 273-281 (2017).

18. Alexander, C. M. O'D., Bowden, R., Fogel, M. L. & Howard, K. T. Carbonate abundances and isotopic compositions in chondrites. *Meteorit. Planet. Sci.* **50**, 810-833 (2015).
19. Fujiya, W. et al. Migration of D-type asteroids from the outer solar system inferred from carbonate in meteorites. *Nat. Astron.* **3**, 910-915 (2019).
20. McCain, K. A. et al. Early fluid activity on Ryugu inferred by isotopic analyses of carbonates and magnetite. *Nat. Astron.***7**, 309-317 (2023).
21. Chacko, T., Cole, D. R. & Horita, J. Equilibrium oxygen, hydrogen and carbon isotope fractionation factors applicable to geologic systems. In *Stable Isotope Geochemistry* (eds. Valley, J. W. and Cole, D. R.) 1-81 (Mineralogical Society of America, 2001).
22. Zolensky, M. E., Bourcier, W. L. & Gooding, J. L. Aqueous alteration on the hydrous asteroids: Results of EQ3/6 computer simulations. *Icarus* **78**, 411-425 (1989).
23. Zheng, Y.-F. On the theoretical calculations of oxygen isotope fractionation factors for carbonate-water systems. *Geochem. J.* **45**, 341-354 (2011).
24. Clayton, R. N. & Mayeda, T. K. The oxygen isotope record in Murchison and other carbonaceous chondrites. *Earth Planet. Sci. Lett.* **67**, 151-161 (1984).
25. Marrocchi, Y., Bekaert, D. V. & Piani, L. Origin and abundance of water in carbonaceous asteroids. *Earth Planet. Sci. Lett.* **482**, 23-32 (2018).
26. Sakamoto, N. et al. Remnants of the early Solar System water enriched in heavy oxygen isotopes. *Science* **317**, 231-233 (2007).
27. Vacher, L. G., Marrocchi, Y., Verdier-Paoletti, M. J., Villeneuve, J. & Gounelle, M. Inward radial mixing of interstellar water ices in the solar protoplanetary disk. *Astrophys. J.* **827**, L1 (2016).
28. Kawasaki, N. et al. Oxygen isotopes of anhydrous primary minerals show kinship between steroid Ryugu and comet 81P/Wild2. *Sci. Adv.* **8**, eade2067 (2022).
29. Wilson L., Keil, K., Browning, L. B., Krot, A. N. & Bourcier, W. Early aqueous alteration, explosive disruption, and reprocessing of asteroids. *Meteorit. Planet. Sci.* **34**, 541-557 (1999).
30. Beck, P. et al. The redox state of iron in the matrix of CI, CM and metamorphosed CM chondrites by XANES spectroscopy. *Geochim. Cosmochim. Acta* **99**, 305-316 (2012).
31. Barnaby, R. J. & Rimstidt, J. D. Redox conditions of calcite cementation interpreted from Mn and Fe contents of authigenic calcites. *Geol. Soc. Am. Bull.* **101**, 795-804.
32. Fujiya, W., Aoki, Y., Ushikubo, T., Hashizume, K. & Yamaguchi, A. Carbon isotopic evolution of aqueous fluids in CM chondrites: Clues from *in-situ* isotope analyses within calcite grains in Yamato-791198. *Geochim. Cosmochim. Acta* **274**, 246-260 (2020).
33. Mumma, M. J. & Charnley, S. B. The chemical composition of comets—Emerging taxonomies and natal heritage. *Annu. Rev. Astron. Astrophys.* **49**, 471–524 (2011).
34. Ootsubo, T. et al. AKARI Near-infrared spectroscopic survey for CO_2 in 18 comets. *Astrophys.*

J. **752**, 15 (2012).

35. Richet, P., Bottinga, Y. & Javoy, M. A review of hydrogen, carbon, nitrogen, and chlorine stable isotope fractionation among gaseous molecules. *Ann. Rev. Earth Planet. Sci.* **5**, 65-110 (1977).
36. Fujiya, W., Sugiura, N., Sano, Y. and Hiyagon, H. Mn–Cr ages of dolomites in CI chondrites and the Tagish Lake ungrouped carbonaceous chondrite. *Earth Planet. Sci. Lett.* **362**, 130-142 (2013).
37. Thiagarajan, N. et al. Isotopic evidence for quasi-equilibrium chemistry in thermally mature natural gases. *Proc. Natl Acad. Sci. USA* **117**, 3989-3995 (2017).
38. Telus, M., Alexander, C. M. O'D., Hauri, E. H. & Wang, J. Calcite and dolomite formation in the CM parent body: Insight from *in-situ* C and O isotope analyses. *Geochim. Cosmochim. Acta* **260**, 275-291 (2019).
39. Vacher, L. G., Marrocchi, Y., Villeneuve, J., Verdier-Paoletti, M. J. & Gounelle, M. Petrographic and C & O isotopic characteristics of the earliest stages of aqueous alteration of CM chondrites. *Geochim. Cosmochim. Acta* **213**, 271-290 (2017).
40. Sheppard, S. M. F. & Schwarcz, H. P. Fractionation of carbon and oxygen isotopes and magnesium between coexisting metamorphic calcite and dolomite. *Contr. Mineral. Petrol.* **26**, 161-198 (1970).
41. Romanek, C. S., Grossman, E. L. & Morse, J. W. Carbon isotopic fractionation in synthetic aragonite and calcite: Effects of temperature and precipitation rate. *Geochim. Cosmochim. Acta* **56**, 419-430 (1992).
42. Aponte, J. C., McLain, H. L., Dworkin, J. P. & Elsila, J. E. Aliphatic amines in Antarctic CR2, CM2, and CM1/2 carbonaceous chondrites. *Geochim. Cosmochim. Acta* **189**, 296-311 (2016).
43. Hässig, M. et al. Isotopic composition of CO_2 in the coma of 67P/Churyumov-Gerasimenko measured with ROSINA/DFMS. *Astron. Astrophys.* **605**, A50 (2017).
44. Yurimoto, H. & Kuramoto, K. Molecular cloud origin for the oxygen isotope heterogeneity in the solar system. *Science* **305**, 1763-1766.
45. Lyons, J. R. & Young, E. D. CO self-shielding as the origin of oxygen isotope anomalies in the early solar nebula. *Nature* **435**, 317-320.
46. Lyons, J. R., Gharib-Nezhad, E. & Ayres, T. R. A light carbon isotope composition for the Sun. *Nat. Commun.* **9**, 908 (2018).
47. Visser, R., van Dishoeck, E. F. & Black, J. H. The photodissociation and chemistry of CO isotopologues: applications to interstellar clouds and circumstellar disks. *Astron. Astrophys.* **503**, 323-353 (2009).
48. Woods, P. M. & Willacy, K. Carbon isotope fractionation in protoplanetary disks. *Astrophys. J.* **693**, 1360-1378 (2009).

Methods

Isotope measurement using ion microprobe

We produced the polished sections of Ryugu samples A0058-C1001 and C0002-C1001, and Ivuna embedded in epoxy[8,28]. The polished sections were coated with a thin (~5 nm) gold film using a Leica EM ACE600 coater at Hokkaido University for backscattered electron (BSE) and X-ray imaging, and elemental analysis before *in-situ* O and C isotope measurements. We observed their mineralogy and petrology and located carbonate grains using a field-emission scanning electron microscope (FE-SEM; JEOL JSM-7000F) equipped with an energy dispersive X-ray spectrometer (EDS; Oxford X-Max 150) at Hokkaido University. The beam currents were ~2 nA and ~1 nA for the X-ray mapping and quantitative analysis, respectively. Quantitative calculations were conducted using Oxford AZtec software.

We selected five and four dolomite grains from the Ryugu samples A0058 and C0002, respectively, and nine calcite grains from C0002 for isotope analyses. We also analysed seven dolomite grains and ten calcite grains from Ivuna. Before the isotope analyses, the samples were coated again with an additional thin (~65 nm) gold film.

We conducted the O and C isotope measurements of the selected carbonate grains using secondary ion mass spectrometry (SIMS; CAMECA ims-1280HR) at Hokkaido University. Instrumental mass fractionation (IMF) was corrected using the UWC3 calcite standard and a series of dolomite-ankerite standards from the WiscSIMS laboratory for calcite and dolomite, respectively[49-51]. Measurement spots were observed using the FE-SEM after the SIMS measurements and data from spots with inclusions or overlapping matrix minerals were rejected. The reported uncertainties (2σ) of isotope compositions are the larger of the external reproducibility, i.e., 2 standard deviation (2SD) of standard measurements or internal precision, i.e., 2 standard error (2SE) of data within single measurements of unknown samples.

The procedures of O isotope measurement of dolomite were described by a previous study[8]. For O isotope measurement of calcite, as previously described for the O isotope measurement of olivine[28], secondary $^{16}O^-$, $^{17}O^-$, and $^{18}O^-$ ions produced by a Cs^+ primary ion beam (~30 pA, ~3 μm) were simultaneously collected using Faraday cup (FC: 10^{11} Ω), electron multiplier (EM), and EM detectors, respectively. Mass resolving power was >6000 sufficient to resolve $^{17}O^-$ from $^{16}OH^-$. The secondary ion intensities of $^{16}O^-$ were 2-3 × 10^7 cps. The measurement time was 240 seconds. The $^{16}OH^-$ count rate was measured immediately after each measurement, and we made a small tail correction on $^{17}O^-$; its contribution to $^{17}O^-$ was typically less than ~0.1‰ and up to ~0.5‰ for a few analyses. The typical uncertainties of $\delta^{17}O$, $\delta^{18}O$, and $\Delta^{17}O$ values were 1.4, 0.9, and 1.4‰, respectively.

For C isotope measurement of dolomite, secondary $^{12}C^-$ and $^{13}C^-$ ions produced by a Cs^+ primary ion (~50 pA, ~2 μm) were simultaneously collected using FC (10^{12} Ω) and EM detectors, respectively. We scanned the primary ion beam across 1 × 1 μm-sized areas to make the SIMS pits shallower and suppress ratio drifts during measurements. Mass resolving power was ~4500, sufficient to resolve $^{13}C^-$ from $^{12}CH^-$. The secondary ion intensities of $^{12}C^-$ were 5-6 × 10^5 cps. The measurement time was 480 seconds. The typical uncertainty of $\delta^{13}C$ values was 1.3‰.

For C isotope measurement of calcite, secondary $^{12}C^-$ and $^{13}C^-$ ions produced by a Cs^+ primary ion (~3 pA, ~1 μm) were simultaneously collected using two EM detectors. We scanned the primary ion beam on 1 × 1 μm-sized areas. Mass resolving power was ~4500. The secondary ion intensities of $^{12}C^-$ were ~2 × 10^4 cps. The measurement time was 800 seconds. The typical uncertainty of $\delta^{13}C$ values was 5.1‰. The larger uncertainty of the calcite measurement was due to the smaller primary ion beam intensity than for the dolomite measurement to analyse small calcite grains.

Data availability

All data generated or analysed during this study are included in this published article (and its supplementary information files) and are available via Zenodo (https://doi.org/10.5281/zenodo.7957625). As the initial analysis of Ryugu samples collected by the Hayabusa2 spacecraft, the specimens analysed in this study were allocated to us by JAXA. The Ivuna specimen used in this study was kindly proved by the Natural History Museum, UK.

References:

49. Kozdon, R., Ushikubo, T., Kita, N. T., Spicuzza, M. & Valley, J. W. Intratest oxygen isotope variability in the planktonic foraminifer *N. pachyderma*: Real vs. apparent vital effects by ion microprobe. *Chem. Geol.* **258**, 327-337 (2009).
50. Śliwiński, M. G. et al. Secondary ion mass spectrometry bias on isotope ratios in dolomite–ankerite, Part I: $\delta^{18}O$ matrix effects. *Geostand. Geoanal. Res.* **40**, 157-172 (2015a).
51. Śliwiński, M. G. et al. Secondary ion mass spectrometry bias on isotope ratios in dolomite-ankerite, Part II: $\delta^{13}C$ matrix effects. *Geostand. Geoanal. Res.* **40**, 173-184 (2015b).